

# Finite Element Analysis of Dynamic Mechanical Responses of Aluminum Honeycomb Sandwich Structures Under Low-Velocity Impact

P. F. Liu · X. K. Li · Z. B. Li

Submitted: 4 March 2017 / Published online: 20 October 2017  
© ASM International 2017

**Abstract** Honeycomb sandwich structures, composed of many regularly arranged hexagonal cores and two skins, often show excellent impact performance due to strong energy absorption ability under impact loads. This paper studies dynamic mechanical responses of aluminum honeycomb sandwich structures. Parametric geometry modeling using UG software and finite element analysis using ANSYS explicit dynamics module are performed. Finite difference algorithm based on time-stepping integration is used to get the impact displacement, and stress and strain with time. Effects of different impact velocities, core length and wall thickness on the distributions of plastic stress and strain are also explored. Results show that thinner honeycomb side length and thicker wall thickness lead to stronger impact resistance. This research provides theoretical support for promoting optimal design of lightweight structures against impact loads.

**Keywords** Low-velocity impact · Aluminum honeycomb sandwich structures · Explicit finite element analysis (FEA)

## Introduction

Lightweight honeycomb sandwich structures are generally composed of many regularly arranged hexagonal cores and two skins, and the panel and honeycomb core can be welded and glued. Now, it has been demonstrated this

special structure shows low density, high stiffness and strength, and excellent heat-shielding performance and impact resistance. Thus, they have been widely applied to the areas such as aerospace, marine and transportation.

Research shows that the structural panel provides almost all the bending stiffness and the in-plane tensile strength of sandwich, and core provides the shear stiffness of sandwich [1]. Therefore, how to design honeycomb sandwich shell structure is a key problem. Due to strong energy absorption capacity of honeycomb structures under impact loading, an important fundamental work is to study dynamic mechanical properties of structures under impact loading. In order to reduce the residual effects due to manufacturing process, e.g., consolidation needed by adhesive bonding between the core and skin, different types of aluminum metals are widely used to manufacture the honeycomb structures. Currently, there is some but not much work on the impact properties of aluminum honeycomb structures. Crupi et al. [2] conducted quasi-static bending tests and low-velocity impact tests of aluminum honeycomb structures and studied the failure mechanisms and collapse modes using 3D computed tomography. Hazizan and Cantwell [3] performed low-velocity impact of honeycomb structures with aluminum cores and glassy fiber/epoxy skins. Foo et al. [4] studied the dynamic mechanical responses of aluminum honeycomb structures using 3D finite element analysis. However, these works did not compare the effects of different impact conditions and structure sizes. In order to improve impact resistance and to promote optimal design of structures, it is necessary to perform parametric research on the dynamic responses of honeycomb structures by considering effects of various factors.

This paper first establishes parametric geometry models of honeycomb structures using UG software. Then, these

---

P. F. Liu (✉) · X. K. Li · Z. B. Li  
Institute of Chemical Machinery and Process Equipment, School of Energy Engineering, Zhejiang University, Hangzhou 310027, China  
e-mail: pffiu@zju.edu.cn

models are imported into ANSYS for numerical analysis. Finite difference algorithm based on time-stepping integration is performed in ANSYS software, where small time increment is used to get accurate and stable solutions. Effects of different impact velocities, core length and wall thickness on the distributions of stress and strain are explored.

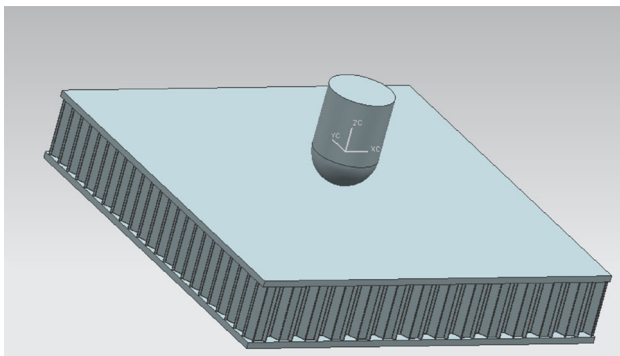
**Finite Element Models and Parameters**

Figure 1 shows the geometry model using UG software which is composed of many regularly arranged hexagonal cores and two skins. Perfect bonding between core and skin is assumed. Materials for core, skin and impactor are AA5052Al, AA5754H32Al and steel, respectively. The material parameters are listed in Table 1. By comparison, three mesh size configurations are used, as listed in Table 2. Finite difference algorithm based on time-stepping integration is used, and a small time increment is set to get accurate and stable solutions. Because the explicit time algorithm requires huge computation time, we select an appropriate mesh size, as shown in Fig. 2. Fixed constraints on four sides of bottom skin are set. The total impact time 0.001 s is assumed. By comparison, six impact velocities 0.5, 1, 2, 4, 6, and 8 m/s are used. Frictional contact between the impactor and top skin surface is set, and augmented Lagrange multiplier algorithm is used for

dynamic contact analysis. Friction coefficient 0.3 is assumed.

**Results and Discussion**

First, numerical results including the curves and distributions are represented by model-3 under 6 m/s impact velocity. Figure 3 shows the maximum Mises equivalent stress–time curve, where the maximum stress increases until a stable value about 430 MPa from about  $1.8e^{-4}$  s. Figure 4 shows the maximum equivalent plastic strain–time curve, where the strain increases always until the maximum value about 0.9 at about time  $5e^{-4}$  s. Figures 5, 6 and 7 show the distributions of equivalent stress, displacement and strain. The top skin deforms severely and impact wave propagates toward adjacent skin. At about time  $1.7e^{-4}$  s, the middle core starts to collapse and the total structures produce severe damage. Secondly, numerical results including the curves and distributions are represented by model-3 under 2 m/s impact velocity. Figures 8 and 9 show the maximum Mises equivalent stress and maximum strain–time curves. Figures 10, 11 and 12 show the distributions of equivalent stress, displacement and strain. By comparison, the structure also produces severe deformation under 2 m/s impact velocity, but does not collapse at about time  $1e^{-3}$  s. Tables 3 and 4 list the maximum stress and strain for three models under different impact velocities. The maximum stress adds gradually with increase in impact velocity from 0.5 to 8 m/s for model-1, and first adds gradually with increase in impact velocity from 0.5 to 2 m/s and then remains basically unchanged after 4 m/s for model-2, and first adds gradually with



**Fig. 1** Geometry model of aluminum honeycomb sandwich structure in UG software

**Table 2** Size parameters for three models

	Radius (mm)	Half wall thickness (mm)	Sandwich height (mm)	Skin thickness (mm)
Model-1	1.2	0.05	2	0.5
Model-2	1.5	0.05	2	0.5
Model-3	1.5	0.08	2	0.5

Where the height of core, skin and impactor is 2, 0.5, and 6.75 mm, respectively

**Table 1** Material parameters for honeycomb structures

	Material	Elastic modulus (MPa)	Poisson’s ratio	Density (kg/m <sup>3</sup> )	Initial yield strength (MPa)	Hardening modulus (MPa)
Core	AA5052A1	$7 \times 10^4$	0.33	2680	200	380
Skin	AA5754H32A1	$7.47 \times 10^4$	0.33	2700	200	380
Impactor	Constructional steel	$1.67 \times 10^5$	0.3	...	...	...

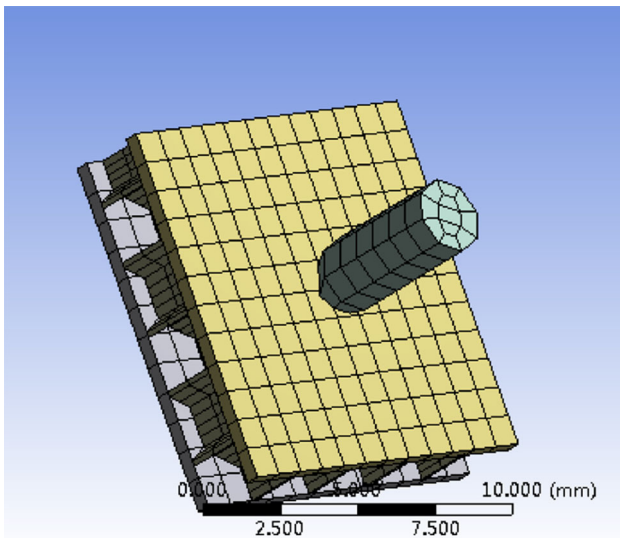


**Fig. 2** Mesh model of aluminum honeycomb sandwich structure in ANSYS software

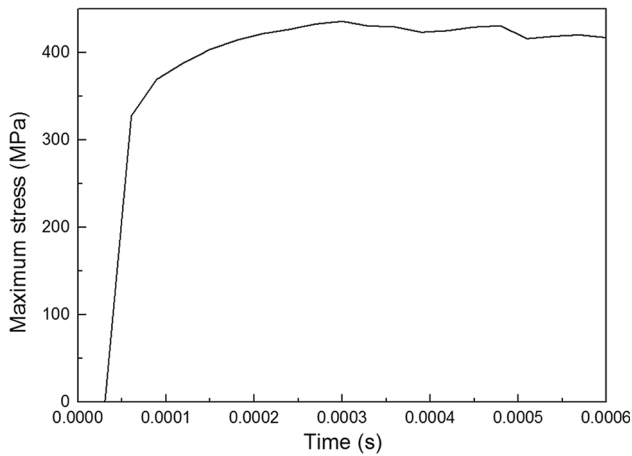


**Fig. 3** Maximum stress–time curve at the impact velocity 6 m/s for model-3

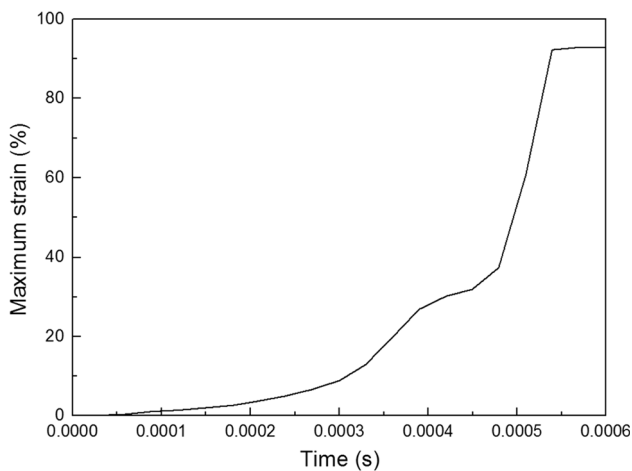


**Fig. 4** Maximum strain–time curve at the impact velocity 6 m/s for model-3

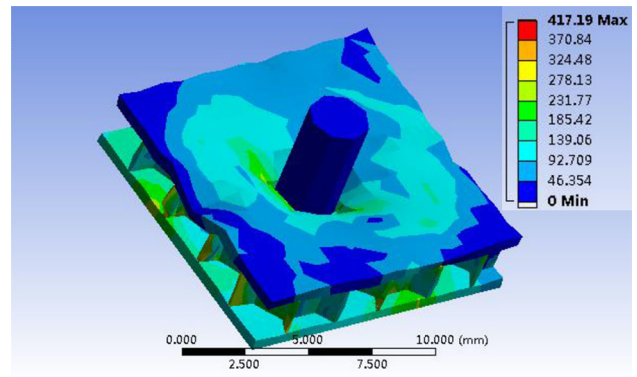


**Fig. 5** Distribution of the equivalent stress at the impact velocity 6 m/s for model-3 at about time  $5e^{-4}$  s

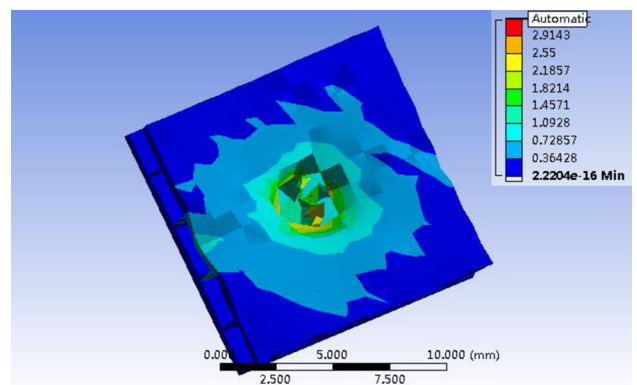


**Fig. 6** Distribution of the displacement at the impact velocity 6 m/s for model-3 at about time  $5e^{-4}$  s

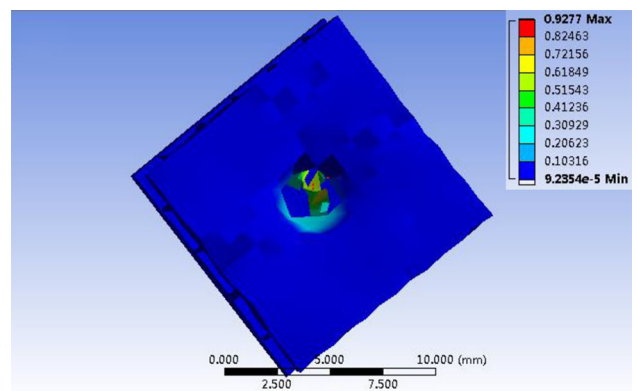


**Fig. 7** Distribution of the equivalent strain at the impact velocity 6 m/s for model-3 at about time  $5e^{-4}$  s

increase in impact velocity from 0.5 to 8 m/s and then decreases little after 4 m/s for model-3. The maximum strain adds gradually with increase in impact velocity from 0.5 to 8 m/s and then decreases little for model-1 and adds always with increase in impact velocity from 0.5 to 8 m/s

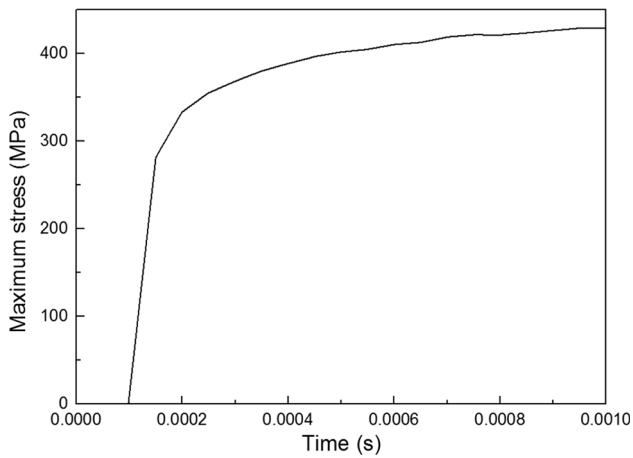


**Fig. 8** Maximum stress–time curve at the impact velocity 2 m/s for model-3

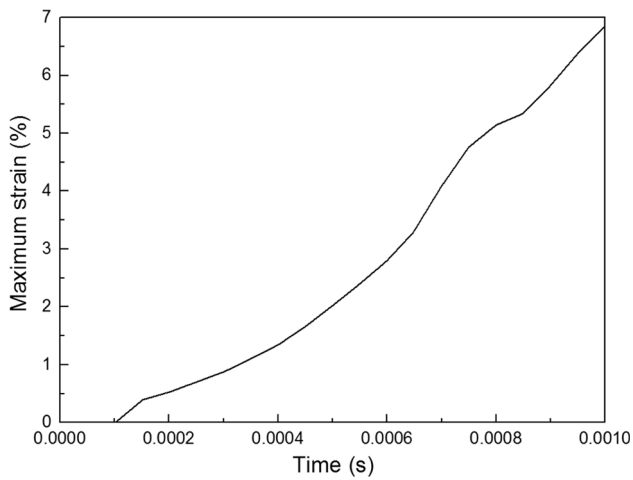


**Fig. 9** Maximum strain–time curve at the impact velocity 2 m/s for model-3

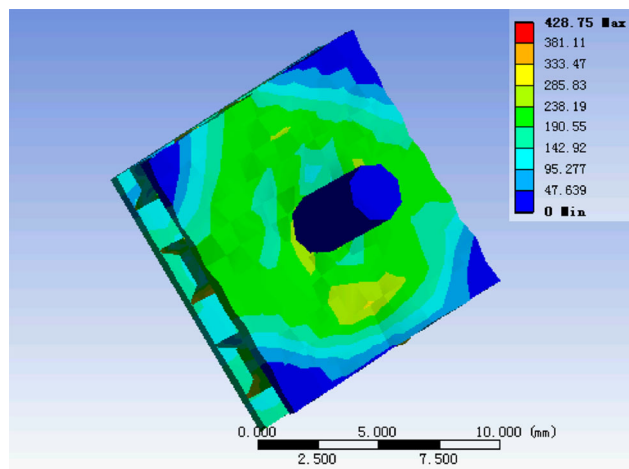


**Fig. 10** Distribution of the equivalent stress at the impact velocity 2 m/s for model-3 at about time  $5e^{-4}$  s

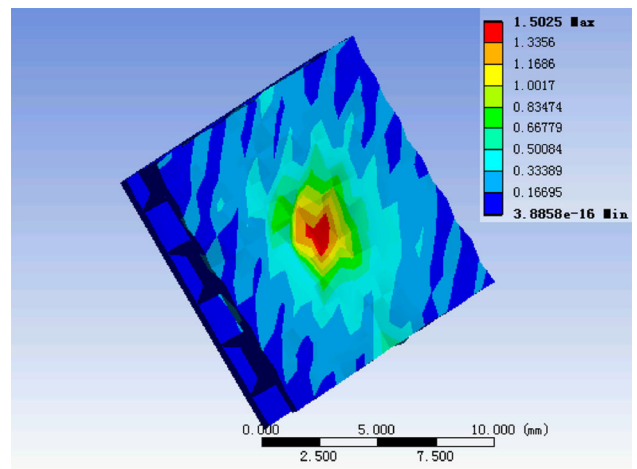


**Fig. 11** Distribution of the displacement at the impact velocity 2 m/s for model-3 at about time  $5e^{-4}$  s

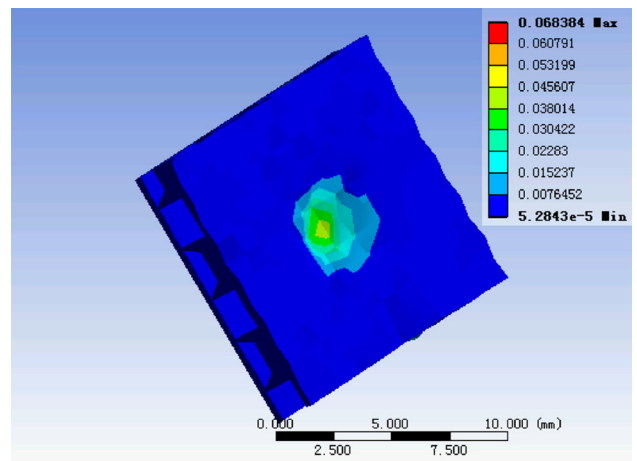


**Fig. 12** Distribution of the equivalent strain at the impact velocity 2 m/s for model-3 at about time  $5e^{-4}$  s

**Table 3** Maximum equivalent stress under impact loading

Impactor velocity (m/s)	0.5	1	2	4	6	8
Maximum equivalent stress in model-1 (MPa)	373.30	383.45	414.92	424.79	430.88	432.37
Maximum equivalent stress in model-2 (MPa)	375.23	384.46	425.98	444.65	444.26	442.98
Maximum equivalent stress in model-3 (MPa)	355.58	387.89	428.75	436.22	435.23	432.86

**Table 4** Maximum equivalent plastic strain under impact loading

Impactor velocity (m/s)	0.5	1	2	4	6	8
Maximum equivalent plastic strain in model-1 (%)	1.05	1.93	12.05	58.69	76.39	64.27
Maximum equivalent plastic strain in model-2 (%)	1.15	1.43	5.89	189.82	146.43	157.98
Maximum equivalent plastic strain in model-3 (%)	0.83	1.69	6.84	58.46	92.77	79.17

**Table 5** Impactor displacement at time  $5 \times 10^{-4}$  s

Impactor velocity (m/s)	0.5	1	2	4	6	8
Displacement in model-1 (mm)	0.2496	0.4635	0.9426	1.9235	2.8816	3.8603
Displacement in model-2 (mm)	0.2499	0.4960	0.9785	1.9464	2.9365	3.9175

**Table 6** Maximum equivalent stress at the impactor displacement 1 mm

Impactor velocity (m/s)	1	2	4	6	8
Maximum equivalent stress in model-1 (MPa)	383.45	399.97	406.07	407.53	410.74
Maximum equivalent stress in model-2 (MPa)	394.46	404.93	412.36	413.22	415.24

**Table 7** Maximum equivalent plastic strain at the impactor displacement 1 mm

Impactor velocity (m/s)	1	2	4	6	8
Maximum equivalent plastic strain in model-1 (%)	1.93	3.05	3.36	3.41	3.51
Maximum equivalent plastic strain in model-2 (%)	2.43	2.71	3.72	3.92	4.58

for model-2, and first adds gradually with increase in impact velocity from 0.5 to 4 m/s and then remains basically unchanged after 4 m/s for model-3.

In the following, we study the effect of honeycomb side length on the impact responses. By comparison, model-1 with side length 1.2 mm and model-2 with side length 1.5 mm are used. Table 5 lists the impactor displacement at time  $5e^{-4}$  s. Model-2 leads to a larger displacement than model-1. Table 6 lists the maximum stress at the impact displacement 1 mm. With the increase in impact velocity from 1 to 8 m/s, the maximum stress increases for both two

**Table 8** Impactor displacement at time  $5 \times 10^{-4}$  s

Impactor velocity (m/s)	1	2	4	6	8
Displacement in model-2 (mm)	0.4960	0.9785	1.9464	2.9365	3.9175
Displacement in model-3 (mm)	0.4941	0.9688	1.9282	2.9175	3.9055

**Table 9** Maximum equivalent stress at the impactor displacement 1 mm

Impactor velocity (m/s)	1	2	4	6	8
Maximum equivalent stress in model-2 (MPa)	394.46	404.93	412.36	413.22	415.24
Maximum equivalent stress in model-3 (MPa)	387.89	400.10	404.11	407.96	410.06

**Table 10** Maximum equivalent plastic strain at the impactor displacement 1 mm

Impactor velocity (m/s)	1	2	4	6	8
Maximum equivalent plastic strain in model-2 (%)	2.43	2.71	3.72	3.92	4.58
Maximum equivalent plastic strain in model-3 (%)	1.69	1.99	2.02	2.60	2.41

models and is larger for model-2 than for model-1 at each velocity. Table 7 lists the maximum strain at the impact displacement 1 mm. Similar results for the maximum strain to the maximum stress are obtained. In addition, the impact displacement for model-2 is also larger than that for model-1, which shows weaker impact resistance ability for model-2 than that for model-1.

Finally, we study the effect of honeycomb wall thickness on the impact responses. By comparison, model-2 with wall thickness 0.1 mm and model-3 with wall thickness 0.16 mm are used. Table 8 lists the impactor displacement at time  $5e^{-4}$  s. Model-2 leads to a larger displacement than model-3. Table 9 lists the maximum stress at the impact displacement 1 mm. With the increase in impact velocity from 1 to 8 m/s, the maximum stress increases for both two models and is larger for model-2 than that for model-3 at each velocity. Table 10 lists the maximum strain at the impact displacement 1 mm. Similar results for the maximum strain to the maximum stress are obtained. In addition, the impact displacement for model-2 is also larger than that for model-3, which shows weaker impact resistance ability for model-2 than that for model-3.

## Conclusions

This paper studies the dynamic mechanical responses of aluminum honeycomb sandwich structures using FEA. Parametric geometry modeling and FEA are performed to study the effects of different impact velocities, honeycomb side length and wall thickness on the stress, strain and displacement of structures. From FEA, three main conclusions are obtained:

1. Stress and strain first add gradually and then tend to led to sudden collapse with the increase in impact energy from 0.5 to 8 m/s.
2. As porous material structures, aluminum honeycomb sandwich structures show distinct size effects for predicting the dynamic mechanical responses. When the specimen sizes are close to the cell sizes, small-size specimen shows different mechanical properties from large-size specimen.
3. Thinner honeycomb side length and thicker wall thickness lead to stronger impact resistance. For

optimization perspective, lightweight design should commit to achieving excellent impact resistance after selecting appropriate side length and wall thickness.

**Acknowledgments** Dr. P.F. Liu would sincerely like to thank for the support by the National Key Fundamental Research and Development Project of China (No. 2015CB057603).

## References

1. J.K. Paika, A.K. Thayamballib, G.S. Kima, The strength characteristics of aluminum honeycomb sandwich panels. *Thin Walled Struct.* **35**, 205–231 (1999)
2. V. Crupi, G. Epasto, E. Guglielmino, Collapse modes in aluminum honeycomb sandwich panels under bending and impact loading. *Int. J. Impact Eng* **43**, 6–15 (2012)
3. MdA Hazizan, W.J. Cantwell, The low velocity impact response of an aluminium honeycomb sandwich structure. *Compos. Part B* **34**, 679–687 (2003)
4. C.C. Foo, L.K. Seah, G.B. Chai, Low-velocity impact failure of aluminium honeycomb sandwich panels. *Compos. Struct.* **85**, 20–28 (2008)